Available online at www.sciencedirect.com
SCIENCE DIRECT
Journal of Photochemistry and Photobiology A: Chemistry 176 (2005) 86–97
Journal of Photochemistry and Photobiology A:Chemistry
www.elsevier.com/locate/jphotochem

The influence of reaction conditions on the photooxidation of diisopropyl ether

E.M. Collins [a], H.W. Sidebottom [a,*], J.C. Wenger [b,**], S. Le Calvé [c,1], A. Mellouki [c], G. LeBras [c], E. Villenave [d], K. Wirtz [e]

[a] *Chemistry Department, University College Dublin, Belfield, Dublin, Ireland*
[b] *Chemistry Department, University College Cork, Cork, Ireland*
[c] *Laboratoire de Combustion et Systèmes Réactifs, CNRS, 45071 Orléans Cedex 2, France*
[d] *Laboratoire de Physico-Chimie Moléculaire, CNRS UMR 5803, Université Bordeaux I, 33405 Talence Cedex, France*
[e] *Fundacion CEAM, C. Charles R. Darwin 14, 46980 Paterna, Valencia, Spain*

Received 15 July 2005; received in revised form 2 September 2005; accepted 7 September 2005
Available online 10 October 2005

Abstract

The hydroxyl radical initiated oxidation of diisopropyl ether has been studied in the large-volume outdoor European Photoreactor (EUPHORE) and in a small, laboratory-based reactor system. The product distributions determined from the experiments were found to be significantly dependent on the reaction conditions and provide strong evidence for the existence of three distinct regimes within the reaction system. In the presence of NO_x, the peroxy radicals react with NO to produce chemically activated $(CH_3)_2CHOC(O)(CH_3)_2$ alkoxy radicals which undergo decomposition by C─C bond scission to yield isopropyl acetate and formaldehyde as the major products. Under conditions where the self-reaction of peroxy radicals dominates, thermoneutral $(CH_3)_2CHOC(O)(CH_3)_2$ radicals are produced, which appear to undergo two reaction pathways; C─C bond scission to yield isopropyl acetate and formaldehyde and isomerisation to form acetone, acetic acid and formaldehyde. Under conditions where the reaction between peroxy and hydroperoxy radicals dominates, unstable hydroperoxides are produced which decompose to yield acetone as the only major reaction product. The results of our study are used to construct chemical mechanisms for the gas-phase photooxidation of diisopropyl ether under various tropospheric conditions.

Keywords: Oxygenated fuel additives; Diisopropyl ether; Atmospheric chemistry; Alkoxy radicals

1. Introduction

Ethers are widely used as fuels additives and solvents. Methyl *tert*-butyl ether (MTBE) is the most common oxygenated fuel additive but other branched ethers, such as ethyl *tert*-butyl ether (ETBE), *tert*-amyl methyl ether (TAME) and diisopropyl ether (DIPE), are also present in certain formulations. The emission of these volatile organic compounds into the atmosphere is an important issue since their oxidation may affect tropospheric ozone levels and also lead to the formation of other secondary pollutants [1]. In order to fully assess the environmental impact of the use of ethers as fuel additives, a detailed understanding of their atmospheric degradation is required. The main atmospheric fate of saturated ethers is gas-phase reaction with hydroxyl radicals [1]. Detailed mechanistic studies on the photooxidation of a range of ethers have been reported in the literature [2] and provide important information on the decomposition pathways available to oxygenated alkoxy radicals.

In this study, the OH radical initiated oxidation of diisopropyl ether (DIPE) has been investigated in the presence and absence of NO_x at the large-volume outdoor European Photoreactor (EUPHORE) [3]. The product distributions in the experiments were found to be significantly dependent on the NO_x concentration thus suggesting the existence of different reaction pathways in the presence and absence of NO_x. Additional experiments have been performed in a laboratory-based reactor under a variety of conditions to elucidate further mechanistic details. The

* Corresponding author. Tel.: +353 1 7162293; fax: +353 1 7162127.
** Corresponding author. Tel.: +353 21 4902454; fax: +353 21 4903014.
E-mail addresses: howard.sidebottom@ucd.ie (H.W. Sidebottom), j.wenger@ucc.ie (J.C. Wenger).
[1] Present address: Centre de Géochimie de la Surface, CNRS et Université Louis Pasteur, 1 rue Blessig, F-67084 Strasbourg, France.

1010-6030/$ – see front matter © 2005 Elsevier B.V. All rights reserved.
doi:10.1016/j.jphotochem.2005.09.004

results of our study are used to construct chemical mechanisms for the gas-phase photooxidation of DIPE under various tropospheric conditions.

2. Experimental

The photooxidation of DIPE was investigated under simulated tropospheric conditions at EUPHORE and also in a small reactor system.

2.1. EUPHORE

The European Photoreactor comprises two large-volume outdoor atmospheric simulation chambers located at the Centro de Estudios Ambientales del Mediterraneo (CEAM) in Valencia, Spain. A detailed description of the installation can be found in the literature [3–7]. The photooxidation of DIPE was performed in a 195 m^3 hemispherical chamber made of Teflon FEP foil and surrounded by a retractable steel housing that is used to control the time of exposure to sunlight. Experiments performed in the presence of NO_x relied upon the in situ production and photolysis of HONO as the source of hydroxyl radicals. For experiments performed in the absence of NO_x, photolysis of hydrogen peroxide was used as the source of hydroxyl radicals. Nitric oxide (Aldrich, 98.5%) and DIPE (Aldrich, 98%) were introduced into the chamber via a stream of purified air, whilst H_2O_2 (Merck, 35 wt.% solution in water) was added to the chamber using a nebuliser.

The loss of reactants and formation of products was monitored using a Nicolet Magna 550 FT-IR spectrometer equipped with a mercury cadmium telluride (MCT) detector. Infrared spectra were obtained by in situ long-path absorption, and were derived from the co-addition of 550 scans recorded using a path length of 553.5 m and a resolution of 1 cm^{-1}. The reactants and products were quantified using calibrated reference spectra which were obtained by introducing known volumes of materials into the chamber. Additional chemical detection was provided by a gas chromatograph (Fisons 8000) equipped with flame ionisation and photoionisation detectors (FID and PID). The chromatograph was operated using a 30 m DB-624 fused silica capillary column (J&W Scientific, 0.32 mm i.d., 1.8 μm film). Air was sampled from the chamber into a 2 cm^3 sampling loop and then injected onto the column. A trace gas analyser (TGA, Fisons), which incorporated a cryogenic enrichment trap coupled to a flame ionisation detector, was also used for chemical analysis of reactants and products. Air samples (200 cm^3) were collected in a sampling loop at 120 °C and passed to a Tenax micro-trap cooled to −120 °C with liquid nitrogen. Injection onto the 30 m DB-1 chromatographic column (J&W Scientific, 0.25 mm i.d., 1.0 μm film) was achieved by rapid heating of the micro-trap to 240 °C.

The concentration of reactants and products decreased through chemical processes and also due to leakage from the chamber. The leak rate in each experiment was determined by adding an unreactive tracer gas (SF_6) to the chamber and measuring its loss by FT-IR spectroscopy. The temperature inside the chamber was continuously monitored using three PT-100 thermocouples and was 303 ± 2 K for all experiments. The intensity of sunlight was measured using two $J(NO_2)$ filter radiometers; the first of which measured direct sunlight and the second faced downwards to measure reflected light from the floor panels. Ozone and NO_x concentrations were continuously monitored using chemiluminescent analysers (Monitor Labs Model 9810A and Eco Physics Model CLD 770 AL, respectively).

2.2. Small reactor

Experiments were performed at 298 ± 2 K and 760 ± 10 Torr of purified air in a collapsible 50 L Teflon reaction vessel [8]. The photooxidation of DIPE was carried out in the absence of NO_x using the photolysis (10 Philips TUV 15 W lamps with an intensity maximum at 254 nm) of H_2O_2 or ozone/water mixtures as the hydroxyl radical source. Measured amounts of reactants were flushed from calibrated Pyrex bulbs into the reaction vessel by a stream of ultra-pure air and the chamber was then filled to its full volume with air. The reactants were allowed to mix for at least 30 min prior to the start of photolysis.

Throughout the course of the reactions, samples of the reaction mixtures were expanded into an evacuable 5 L Teflon coated multipath cell mounted in the sample compartment of an FT-IR spectrometer (Mattson RS series). Infrared spectra were derived from the co-addition of 128 scans recorded using a path length of 9.75 m over the range 500–4000 cm^{-1} with a resolution of 2 cm^{-1}. Products and reactants were identified by comparison of the infrared spectra with those of authentic samples. The possible loss of reactants and products in the dark was measured but found to be negligible over the timescale of the experiments. Reference spectra and calibration curves for reactants and products were obtained by expanding measured pressures of the pure compounds into the IR cell. Complex spectra were analysed by successively subtracting the absorption features of known compounds with the use of calibration spectra.

3. Results

3.1. EUPHORE

A series of experiments was performed at EUPHORE on the photooxidation of DIPE in the presence and absence of NO_x. Data from three of the experiments are presented here and summarised in Table 1. The first experiment was carried out under "classic NO_x" conditions where the initial NO concentration was about one tenth that of the hydrocarbon concentration. In the initial stages of the reaction, the major products detected by FT-IR spectroscopy were isopropyl acetate (IPAc) and formaldehyde. IPAc was also detected and quantified by GC-PID. In the latter stages of the reaction acetone was detected as the major reaction product by GC-PID. Acetone is a relatively weak infrared absorber and was difficult to measure quantitatively using FT-IR spectroscopy. The concentration–time profile and product yield plots are shown in Fig. 1 and clearly indicate that a significant change in product distribution is observed as the NO concentration is depleted during the course of the reaction. In the early stages of the experiment, whilst NO was present

Table 1
Experimental conditions and results for the photooxidation of diisopropyl ether (DIPE) at EUPHORE

Conditions	Classic NO_x	High NO_x	NO_x free
Initial concentrations[a] (ppbV)	[DIPE] = 1200, [NO] = 120, $[NO_2]$ = 27	[DIPE] = 1200, $[NO]_{max}$ = 445	[DIPE] = 1200, $[H_2O_2]$ = 45 000
OH concentration[b] (molecule cm^{-3})	9.05×10^5	4.39×10^5	2.12×10^6
$J(NO_2)_{average}$ ($\times 10^{-3}$ s^{-1})	6.6 ± 0.58	6.0 ± 0.40	3.7 ± 0.13
Maximum product concentrations[a] (ppbV)	[IPAc] = 115, [acetone] = 190, [HCHO] = 195	[IPAc] = 145, [acetone] = 25, [HCHO] = 130	[IPAc] = 15, [acetone] = 460
Product yields[c] (%)	9:30–11:30 h—IPAc = 79 ± 6, acetone = 16 ± 2, HCHO = 110 ± 15; 13:30–15:30 h—IPAc = 0 ± 7, acetone = 93 ± 14, HCHO = 7 ± 5	IPAc = 107 ± 7, acetone = 17 ± 2, HCHO = 89 ± 5	IPAc = 3 ± 1, acetone = 102 ± 4

[a] 1 ppbV = 2.46×10^{10} molecule cm^{-3} at 298 K and 1 atm.
[b] Calculated from the loss of DIPE using $k(OH + DIPE) = 1.04 \times 10^{-11}$ cm^3 molecule s^{-1} [1].
[c] Molar yields relative to DIPE loss corrected for secondary reaction with OH radicals but not photolysis. Errors are twice the standard deviation and represent precision only.

in relatively high concentration, IPAc and formaldehyde were observed as the major products. However, as the concentration of NO decreased due to reactions with peroxy and hydroperoxy radicals, the yields of IPAc and formaldehyde decreased as acetone became a major product. Finally, under very low NO concentrations, acetone appears to be the only product. Although the product yield plot in Fig. 1 shows significant curvature, the average yields of the products during different time

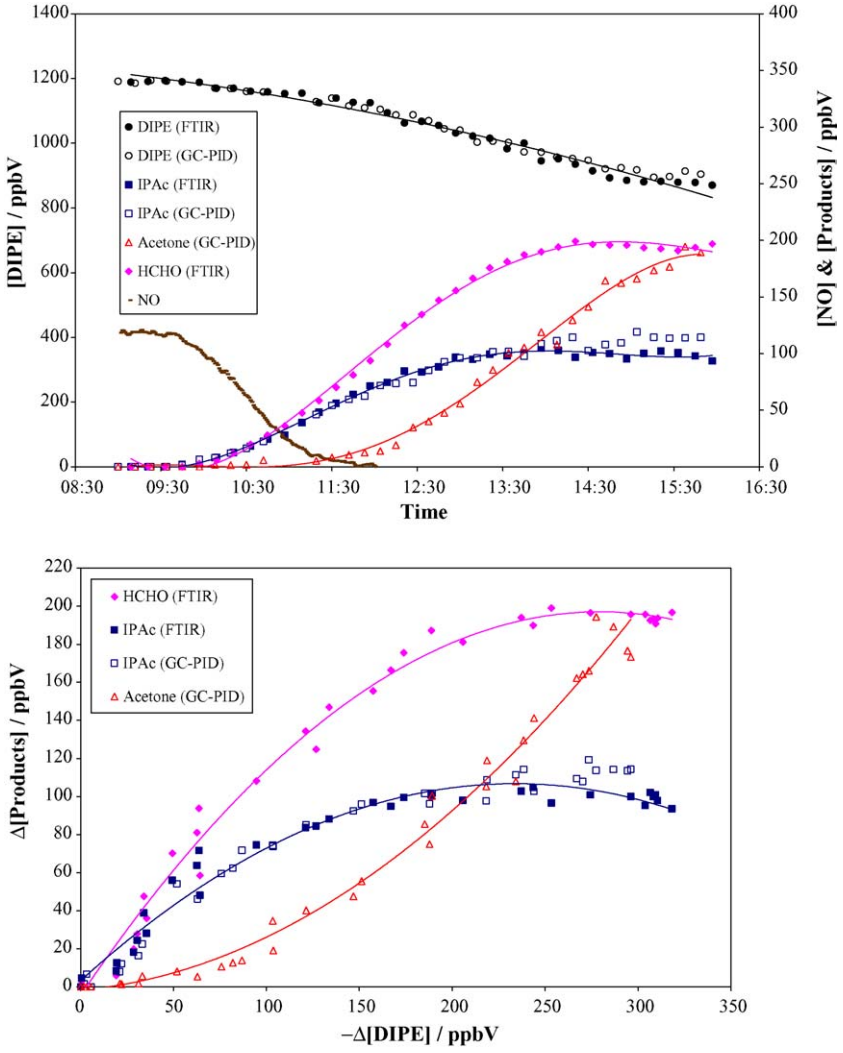

Fig. 1. Concentration–time profile and product yield plot for the photooxidation of DIPE at EUPHORE under "classic NO_x" conditions.

Table 2
Experimental conditions and results for the photooxidation of diisopropyl ether (DIPE) in the small reactor

Conditions	O_3/H_2O	$O_3/H_2O/CH_3OH$	H_2O_2
Initial concentrations[a] (ppmV)	[DIPE] = 70, [O_3] = 50, [H_2O] = 5000	[DIPE] = 32, [O_3] = 50, [H_2O] = 5000, [CH_3OH] = 580	[DIPE] = 71, [H_2O_2] = 2000
Product yields[b] (%)	IPAc = 38 ± 3, acetone = 73 ± 3, acetic acid = 17 ± 1, HCHO = detected	IPAc = 18 ± 2, acetone = 115 ± 8, HCHO = detected	IPAc < 5, acetone = (55–75) ± 9

[a] 1 ppmV = 2.46×10^{13} molecule cm^{-3} at 298 K and 1 atm.
[b] Molar yields relative to DIPE loss corrected for secondary reaction with OH radicals but not photolysis. Errors are twice the standard deviation and represent precision only.

periods of the reaction can be estimated by taking tangents to the curves. The corresponding yields for the initial (9:30–11:30 h) and final (13:30–15:30 h) stages of the reaction are listed in Table 1 and provide strong evidence for the existence of different reaction pathways occurring in the presence and absence of NO. In order to investigate these reaction pathways in isolation, experiments were carried out under "high NO_x" conditions and also in the absence of NO_x using H_2O_2 as the hydroxyl radical precursor.

In the "high NO_x" experiment, NO was continually added to the chamber during the course of the reaction. The trace gas analyser (TGA) was also employed in this experiment to aid detection of the products. The concentration–time profile and product yield plots are shown in Fig. 2. IPAc and HCHO were observed as the major reaction products but the yield of acetone was considerably smaller than in the "classic NO_x" experiment. The third experiment was carried out under "NO_x free" conditions. The concentration–time profile and product yield plots are

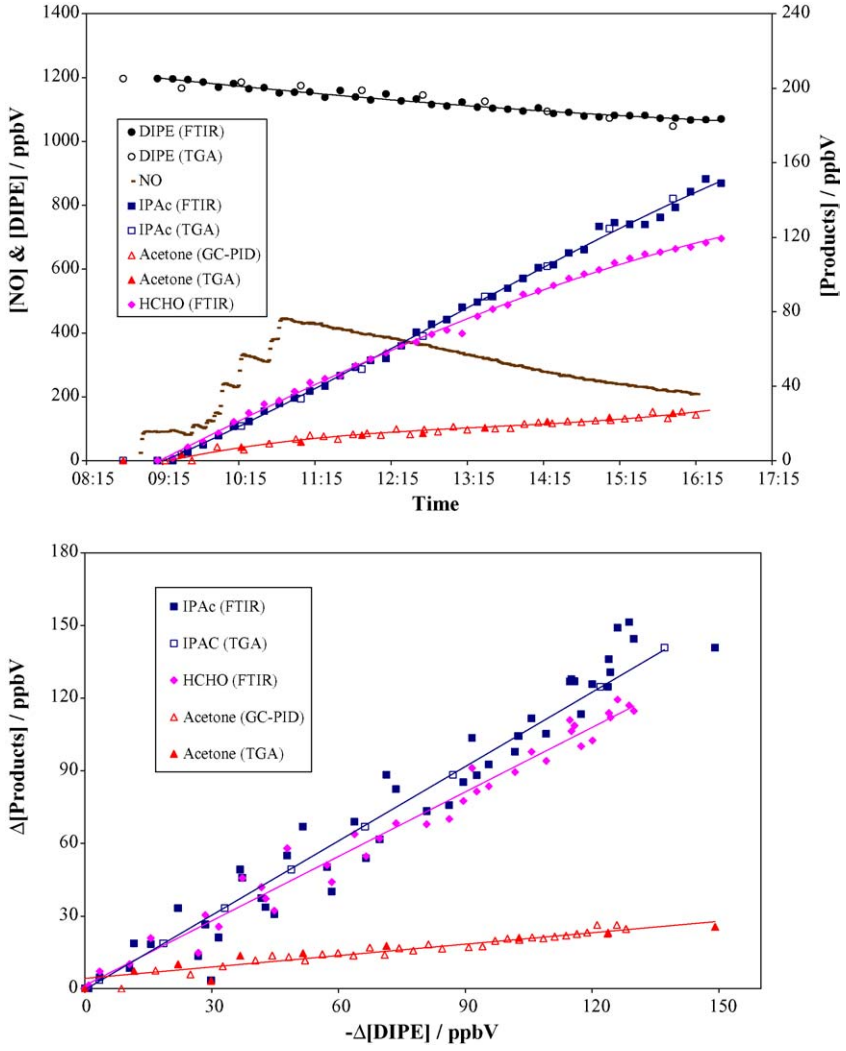

Fig. 2. Concentration–time profile and product yield plot for the photooxidation of DIPE at EUPHORE under "high NO_x" conditions.

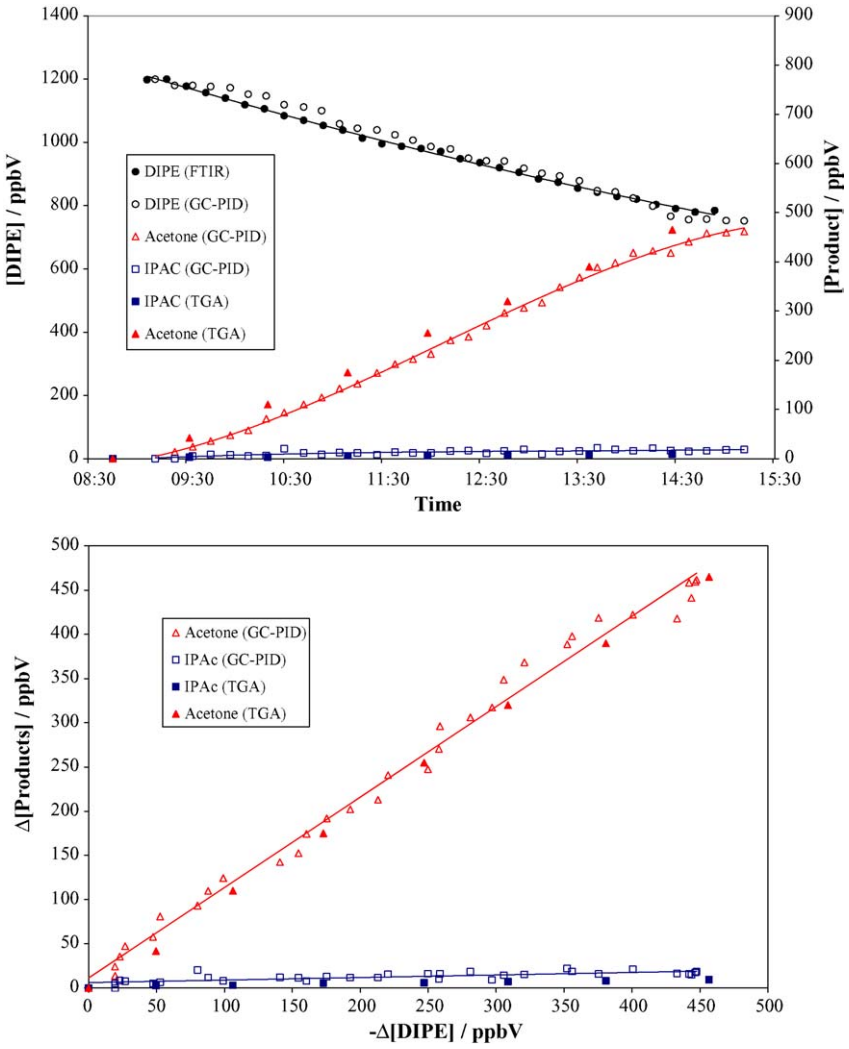

Fig. 3. Concentration–time profile and product yield plot for the photooxidation of DIPE at EUPHORE under "NO_x Free" conditions.

shown in Fig. 3. In this experiment, the identification of products by FT-IR spectroscopy was severely hindered by the presence of saturated absorption bands in the fingerprint region due to the large amount of H_2O_2 and water in the chamber. Consequently, GC-PID and TGA were used to show that acetone and IPAc were the major and minor reaction products, respectively.

3.2. Small reactor

A series of experiments on the photooxidation of DIPE in the absence of NO_x was performed in the small Teflon reactor. Data from three of the experiments are presented here and summarised in Table 2. In the first experiment, carried out using an O_3/H_2O mixture as the OH source, both IPAc and acetone were identified as reaction products along with acetic acid, CH_3COOH. In the second experiment, CH_3OH was added to an O_3/H_2O mixture to increase the HO_2 radical content in the chamber during the reaction. Although IPAc and acetone were present in the FT-IR spectrum of the products, no CH_3COOH was detected. Formaldehyde was also detected in these two experiments, but at very low concentrations since it was rapidly photolysed by the radiation from the UV lamps, as indicated by the presence of CO in the product spectra. The third experiment was carried out using the photolysis of H_2O_2 as the OH radical source; acetone was identified as the major reaction product with trace amounts of IPAc also detected. Product yield plots for the reactions are given in Figs. 4–6. The yield plots for the O_3/H_2O and $O_3/H_2O/CH_3OH$ experiments, shown in Figs. 4 and 5, are all reasonably linear. However, the yield of acetone in the H_2O_2 experiment, Fig. 6, shows pronounced curvature indicating that it may be formed as a secondary product. The estimated yields of acetone for the start and end of the experiment obtained by drawing tangents to the curve are 55% and 75%, respectively. The calculated product yields for all the experiments performed in the small reactor are listed in Table 2.

4. Discussion

The observed product distributions for the OH initiated oxidation of DIPE can be used to elucidate the importance of various possible reaction pathways available to the peroxy and alkoxy radicals generated in the photooxidation system. Initial attack

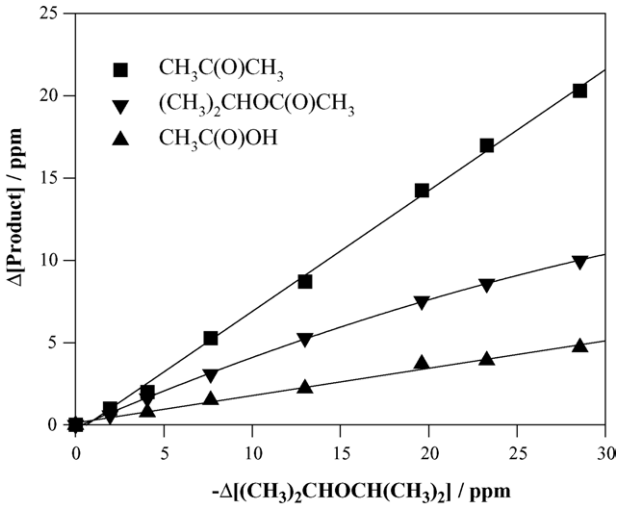

Fig. 4. Plots of product formation against reactant loss for the photolysis of DIPE (70 ppmV), O_3 (~50 ppmV) and H_2O (~5000 ppmV) in air.

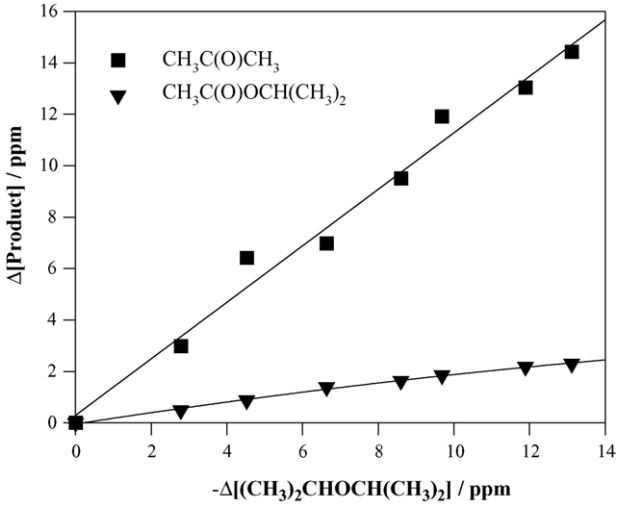

Fig. 5. Plots of product formation against reactant loss for the photolysis of DIPE (32 ppmV), O_3 (~50 ppmV), H_2O (~5000 ppmV) and CH_3OH (580 ppmV) in air.

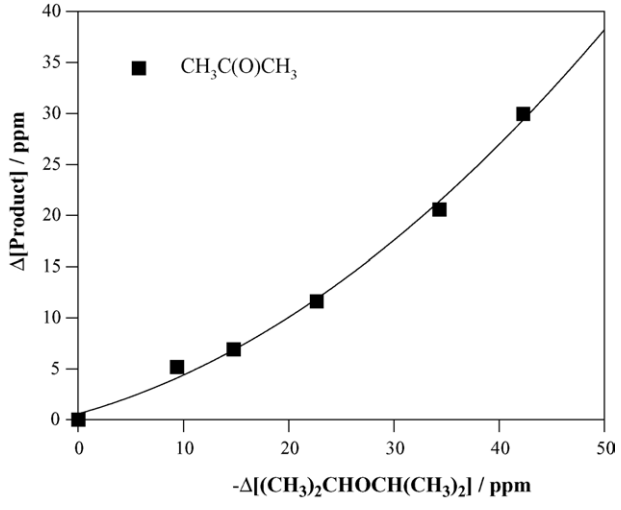

Fig. 6. Plot of product formation against reactant loss for the photolysis of DIPE (71 ppmV) and H_2O_2 (~2000 ppmV) in air.

by OH radicals on DIPE may involve hydrogen atom abstraction from either the >CH– or $-CH_3$ group and results in the formation of two different alkyl radicals:

$$OH + (CH_3)_2CHOCH(CH_3)_2 \rightarrow (CH_3)_2CHOC(CH_3)_2 + H_2O \quad (1a)$$

$$OH + (CH_3)_2CHOCH(CH_3)_2 \rightarrow (CH_3)_2CHOCH(CH_3)CH_2 + H_2O \quad (1b)$$

As discussed by Wallington et al. [9], H-atom abstraction from the $-CH_3$ group in DIPE is of minor importance and reaction (1a) is thus the dominant reaction pathway. The alkyl radical $(CH_3)_2CHOC(CH_3)_2$ reacts rapidly with O_2 to form the corresponding peroxy radical:

$$(CH_3)_2CHOC(CH_3)_2 + O_2 + M \rightarrow (CH_3)_2CHOC(O_2)(CH_3)_2 + M \quad (2)$$

The fate of the peroxy radical depends on the availability of NO_x in the reaction system.

4.1. Photooxidation of DIPE in the presence of NO_x

In the presence of NO_x, the peroxy radical undergoes reaction with NO to form the corresponding alkoxy radical:

$$(CH_3)_2CHOC(O_2)(CH_3)_2 + NO \rightarrow (CH_3)_2CHOC(O)(CH_3)_2 + NO_2 \quad (3)$$

The alkoxy radical, $(CH_3)_2CHOC(O)(CH_3)_2$, formed in reaction (3) can undergo several possible reactions including C–C and C–O bond fission and isomerisation [10]:

$$(CH_3)_2CHOC(O)(CH_3)_2 \rightarrow (CH_3)_2CHOC(O)CH_3 + CH_3 \quad (4a)$$

$$(CH_3)_2CHOC(O)(CH_3)_2 \rightarrow CH_3C(O)CH_3 + (CH_3)_2CHO \quad (4b)$$

$$(CH_3)_2CHOC(O)(CH_3)_2 \rightarrow CH_2CH(CH_3)OC(OH)(CH_3)_2 \quad (4c)$$

$$(CH_3)_2CHOC(O)(CH_3)_2 \rightarrow (CH_3)_2COC(OH)(CH_3)_2 \quad (4d)$$

Decomposition by C–C bond fission, reaction (4a), produces isopropyl acetate and a methyl radical which subsequently reacts with O_2 and NO to yield formaldehyde:

$$CH_3 + O_2 + M \rightarrow CH_3O_2 + M \quad (5)$$

$$CH_3O_2 + NO \rightarrow CH_3O + NO_2 \quad (6)$$

$$CH_3O + O_2 \rightarrow HCHO + HO_2 \quad (7)$$

Decomposition of the alkoxy radical $(CH_3)_2CHOC(O)(CH_3)_2$ via C–O bond fission, reaction (4b), gives acetone and the

$(CH_3)_2CHO$ radical which generates a further molecule of acetone by reaction with O_2:

$$(CH_3)_2CHO + O_2 \rightarrow CH_3C(O)CH_3 + HO_2 \quad (8)$$

Isomerisation of the alkoxy radical $(CH_3)_2CHOC(O)(CH_3)_2$ can occur via a 1,5-H-atom shift reaction, reaction (4c) [10]. The resulting alkyl radical reacts with O_2 and NO to yield the corresponding alkoxy radical:

$$CH_2CH(CH_3)OC(OH)(CH_3)_2 + O_2 + M \; rm\rightarrow \; O_2CH_2CH(CH_3)OC(OH)(CH_3)_2 + M \quad (9)$$

$$O_2CH_2CH(CH_3)OC(OH)(CH_3)_2 + NO \; rm\rightarrow \; OCH_2CH(CH_3)OC(OH)(CH_3)_2 + NO_2 \quad (10)$$

The alkoxy radical, $OCH_2CH(CH_3)OC(OH)(CH_3)_2$, is structurally similar to that formed following OH radical addition at the two-position in propene in the presence of O_2, i.e. $OCH_2CH(CH_3)OH$, which has been shown to decompose mainly by C–C bond cleavage [10] rather than react with O_2. Therefore, the major decomposition pathway of $OCH_2CH(CH_3)OC(OH)(CH_3)_2$ is also likely to be C–C bond cleavage:

$$OCH_2CH(CH_3)OC(OH)(CH_3)_2 \rightarrow CH(CH_3)OC(OH)(CH_3)_2 + HCHO \quad (11)$$

The alkyl radical formed in reaction (11) will rapidly add O_2 to form a peroxy radical and subsequently react with NO to produce the corresponding alkoxy radical, $OCH(CH_3)OC(OH)(CH_3)_2$. This radical is similar in structure to that formed following H-atom abstraction from the $-CH_2-$ group in diethyl ether, i.e. $OCH(CH_3)OCH_2CH_3$, which mainly decomposes by C–C bond fission to form ethyl formate ($HC(O)OC_2H_5$) [11–14]. It is reasonable to assume, therefore, that $OCH(CH_3)OC(OH)(CH_3)_2$ also decomposes by C–C bond fission:

$$OCH(CH_3)OC(OH)(CH_3)_2 \rightarrow HC(O)OC(OH)(CH_3)_2 + CH_3 \quad (12)$$

The product, $HC(O)OC(OH)(CH_3)_2$, is a hemiacylal, which is unstable and would dissociate to produce formic acid and acetone [15]. Thus, isomerisation of the alkoxy radical $(CH_3)_2CHOC(O)(CH_3)_2$ by a 1,5-H-atom shift reaction is expected to produce acetone and formic acid with yields of 100% and formaldehyde with a molar yield of 200%.

Alkoxy radical isomerisation reactions proceed via a cyclic transition state. The 1,5-H-atom shift isomerisation reaction is expected to be favourable because it can proceed through a 6-membered ring structure [10]. Isomerisation reactions involving a 1,4-H-atom shift are calculated to be much less important because of the ring strain involved in a five-membered ring transition state. However, there is some evidence in the literature to support the feasibility of a 1,4-H-atom shift reaction, particularly for oxygenated alkoxy radicals. Theoretical investigations on the alkoxy radicals formed following OH radical addition to ethene and propene have shown that their most stable conformations contain intramolecular hydrogen bonds [16–18], which are formed via a five-membered ring. Both five- and six-membered ring transition states are possible for $(CH_3)_2CHOC(O)(CH_3)_2$. Since the electron withdrawing effect of the ether oxygen is greater on the tertiary H-atom of the isopropyl group than on the primary H-atoms, the tertiary H-atom has a higher partial positive charge. Hydrogen bonding via a five-membered ring is therefore likely to be favoured and if it occurred would lower the energy barrier to 1,4-H-atom shift isomerisation. This would counteract the extra ring strain involved in the five-membered ring and may explain why isomerisation could occur in this case:

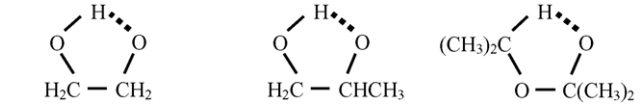

alkoxy radical formed from OH addition to ethene | alkoxy radical formed from OH addition to propene | alkoxy radical formed in reaction (3)

The 1,4-H-atom shift isomerisation of the alkoxy radical $(CH_3)_2CHOC(O)(CH_3)_2$, reaction (4d), produces an alkyl radical which will be rapidly oxidised to form the corresponding alkoxy radical $(CH_3)_2C(O)OC(OH)(CH_3)_2$ that can decompose by either C–C or C–O bond fission:

$$(CH_3)_2C(O)OC(OH)(CH_3)_2 \rightarrow CH_3C(O)OC(OH)(CH_3)_2 + CH_3 \quad (13a)$$

$$(CH_3)_2C(O)OC(OH)(CH_3)_2 \rightarrow CH_3C(O)CH_3 + HOC(O)(CH_3)_2 \quad (13b)$$

C–C bond cleavage yields a CH_3 radical, which is converted to formaldehyde, and a hemiacylal which is expected to dissociate to form acetic acid and acetone [15]:

$$CH_3C(O)OC(OH)(CH_3)_2 \rightarrow CH_3C(O)OH + CH_3C(O)CH_3 \quad (14)$$

C–O bond cleavage yields a molecule of acetone and the $HOC(O)(CH_3)_2$ radical which will cleave a C–C bond to form acetic acid and a methyl radical which is oxidised to formaldehyde:

$$HOC(O)(CH_3)_2 \rightarrow CH_3C(O)OH + CH_3 \quad (15)$$

Thus, C–C and C–O fission of the alkoxy radical $(CH_3)_2C(O)OC(OH)(CH_3)_2$ would produce the same reaction products. Consequently, isomerisation of the alkoxy radical $(CH_3)_2CHOC(O)(CH_3)_2$ by a 1,4-H-atom shift reaction is expected to produce acetone, acetic acid and formaldehyde with yields of 100%.

The relative importance of the four competing reaction pathways for the alkoxy radical $(CH_3)_2CHOC(O)(CH_3)_2$ can be determined from the product yields obtained for the photooxidation of DIPE in the presence of NO_x. In the experiment performed under "high NO_x" conditions, Fig. 2, both IPAc and formaldehyde were formed with yields of around 100%,

and only relatively small amounts of acetone were detected. Similarly during the initial period (9:30–11:30 h) of the "classic NO_x" experiment, Fig. 1 and Table 1, the yields of IPAc and formaldehyde were also very high, with only a small amount of acetone detected. These data agree with the findings of the only previously published work on DIPE photooxidation by Wallington et al. [9], where, in the presence of excess NO, the yield of IPAc was also found to be close to 100% (within experimental error). Consequently, it can be concluded that, when the alkoxy radical $(CH_3)_2CHOC(O)(CH_3)_2$ is generated from the reaction of the corresponding peroxy radical with NO, its major fate is C–C bond fission to produce IPAc and methyl radicals which are oxidised to formaldehyde. Although IPAc and formaldehyde are expected to be produced in equal amounts, the data shown in Fig. 2 indicates that the yield of formaldehyde decreases slightly as the experiment progresses. Since the concentrations of IPAc and formaldehyde have been corrected for secondary reaction with OH radicals, this suggests that formaldehyde also undergoes another loss process, probably photolysis.

The detection of small amounts of acetone during the photooxidation of DIPE in the presence of NO_x suggests that at least one of the other reaction pathways is occurring to a small extent. C–O bond fission of the $(CH_3)_2CHOC(O)(CH_3)_2$ radical via reactions (4b) and (8) would produce two molecules of acetone. However, the decomposition of alkoxy radicals by C–O bond fission to form a further alkoxy radical are calculated, using the estimation methods of Atkinson [10], to be slow and of little importance. Nevertheless, there is some experimental evidence to indicate that for oxygenated alkoxy radicals, C–O bond fission is in fact competitive with C–C bond fission [11,12,19–21] and hence C–O bond fission of the $(CH_3)_2CHOC(O)(CH_3)_2$ radical cannot be ruled out as the source of acetone. Isomerisation of the $(CH_3)_2CHOC(O)(CH_3)_2$ radical can also lead to the formation of acetone and is expected to be more energetically favourable than C–O bond fission [10]. The 1,5-H-atom shift reaction generates formaldehyde and formic acid as co-products, whilst the 1,4-H-atom shift reaction, also produces formaldehyde and acetic acid. Thus, formic acid and acetic acid are potentially useful markers for the existence of reactions (4c) and (4d), respectively. No evidence to support the formation of formic or acetic acid was obtained in the experiments carried out in the presence of NO_x. However, this does not necessarily rule out isomerisation reactions as the source of acetone since the low yields expected for the compounds, coupled with the poor sensitivity of GC and FT-IR spectroscopy for the detection of organic acids, means that the acids could be formed at levels below the detection limits of the available analytical techniques. Indeed, as discussed below, the identification of acetic acid amongst the products in the small reactor experiments provides evidence for isomerisation of the $(CH_3)_2CHOC(O)(CH_3)_2$ radical via a 1,4-H-atom shift. As a result, it seems most likely that the formation of acetone during the photooxidation of DIPE in the presence of NO_x can be attributed to this reaction. Based on the results obtained in this work, a simplified mechanism for the photooxidation of DIPE in the presence of NO_x has been constructed and is shown in Fig. 7.

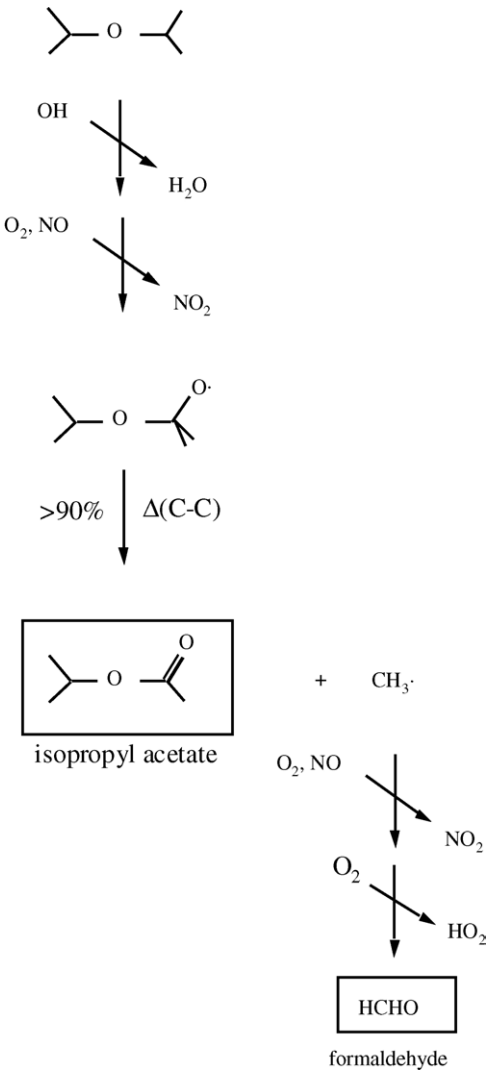

Fig. 7. Mechanism for the oxidation of diisopropyl ether in the presence of NO_x.

4.2. Photooxidation of DIPE in the absence of NO_x

In the absence (or at low levels) of NO_x, peroxy–peroxy ($RO_2 + RO_2$) and peroxy–hydroperoxy ($RO_2 + HO_2$) radical reactions can take place. Since H-atom abstraction from the >CH– group in DIPE dominates, $(CH_3)_2CHOC(O_2)(CH_3)_2$ is the major peroxy radical within the reaction system. The self-reaction of $(CH_3)_2CHOC(O_2)(CH_3)_2$ can only occur via the alkoxy channel because there is no H atom on the carbon atom adjacent to the radical site:

$$2(CH_3)_2CHOC(O_2)(CH_3)_2 \rightarrow 2(CH_3)_2CHOC(O)(CH_3)_2 + O_2 \quad (16)$$

The peroxy radical formed can also react with hydroperoxy radicals to form a hydroperoxide:

$$(CH_3)_2CHOC(O_2)(CH_3)_2 + HO_2 \rightarrow (CH_3)_2CHOC(O_2H)(CH_3)_2 + O_2 \quad (17)$$

A series of experiments were carried out in the small reactor system to elucidate further mechanistic details on the photooxidation of DIPE in the absence of NO_x. The reaction conditions were designed to study the two possible fates of the peroxy radical $(CH_3)_2CHOC(O_2)(CH_3)_2$, i.e. reaction with another peroxy radical and reaction with the hydroperoxy radical. In the OH radical initiated oxidation performed using the O_3/H_2O mixture, the peroxy radical self-reactions are expected to dominate since any HO_2 radicals formed can also react with O_3, which is present at much greater concentrations than RO_2:

$$HO_2 + O_3 \rightarrow HO + 2O_2 \quad (18)$$

Under these conditions, isopropyl acetate, acetone, acetic acid and formaldehyde were all produced (Fig. 4 and Table 2). The product distribution is significantly different to that observed for experiments performed in the presence of NO_x as acetone is formed in a considerably higher yield and the amount of IPAc produced is more than halved. This indicates that, for $(CH_3)_2CHOC(O)(CH_3)_2$ radicals generated from the peroxy radical self-reaction, isomerisation via a 1,4-H-atom shift is more favourable than C–C bond fission.

The addition of methanol to the O_3/H_2O mixture acted as an extra source of HO_2 radicals:

$$OH + CH_3OH \rightarrow H_2O + CH_2OH \quad (19)$$

$$CH_2OH + O_2 \rightarrow HCHO + HO_2 \quad (20)$$

Under these conditions the peroxy radical is likely to undergo both self-reaction and reaction with HO_2, reactions (16) and (17), respectively. IPAc and acetone were detected in the infrared spectra of the reaction products but acetic acid was not observed (Fig. 5 and Table 2). The lower yield of IPAc and the absence of acetic acid confirms that the peroxy radical self-reaction is occurring to a lesser extent than in the O_3/H_2O experiment and that acetone is a likely product of the $RO_2 + HO_2$ reaction.

For experiments performed in the small reactor and at EUPHORE using the photolysis of H_2O_2 as the OH radical source, only trace amounts of IPAc were detected and acetone was observed as the only major reaction product (Figs. 3 and 5, Tables 1 and 2). Under these conditions $RO_2 + HO_2$ radical reactions are likely to dominate since the OH radicals produced can react with the large amount of H_2O_2 present to produce HO_2:

$$OH + H_2O_2 \rightarrow H_2O + HO_2 \quad (21)$$

As indicated in reaction (17), the reaction of the peroxy radical with HO_2 produces the hydroperoxide, $(CH_3)_2CHOC(O_2H)(CH_3)_2$. No evidence for this compound was found in the FT-IR spectra obtained in the small reactor and at EUPHORE. However, as described above, the characteristic absorption bands for hydroperoxides would be obscured by those of H_2O_2 and water, which are present in much larger quantities in the chambers. In addition, hydroperoxides are reactive species and may be lost in the chamber via photolysis, reaction with OH radicals or decomposition. Photolysis would result in cleavage of the O–O bond to produce the alkoxy radical $(CH_3)_2CHOC(O)(CH_3)_2$ and OH. This radical would be expected to yield IPAc, acetone and acetic acid in yields similar to those observed in the O_3/H_2O experiment. However, the absence of acetic acid and formaldehyde in the product spectra, along with the low yield observed for IPAc suggests that photolysis of the hydroperoxide is of minor importance. Reaction of the hydroperoxide with OH radicals would involve H-atom abstraction from either the $-O_2H$ group or the tertiary C–H bond. Attack at the $-O_2H$ group would produce the peroxy radical $(CH_3)_2CHOC(O_2)(CH_3)_2$, which would simply react with HO_2 to reform the hydroperoxide, reaction (17). Attack at the tertiary C–H bond would produce an alkyl radical which would be rapidly oxidised to form the corresponding peroxy radical $(CH_3)_2C(O_2)OC(O_2H)(CH_3)_2$, which is likely to react with HO_2 to form a di-hydroperoxide:

$$(CH_3)_2C(O_2)OC(O_2H)(CH_3)_2 + HO_2 \rightarrow (CH_3)_2C(O_2H)C(O_2H)(CH_3)_2 + O_2 \quad (22)$$

Very little information is available concerning the stability of this type of compound. However, it is possible that the compound may decompose, undergo photolysis or react with OH radicals to produce acetone.

The other possible reaction pathway for the hydroperoxide formed in reaction (17) is decomposition. This compound is similar in structure to 1-hydroxyalkyl hydroperoxides, HOCH(OOH)R, which are unstable and are known to decompose to H_2O_2 and an aldehyde, RCHO [22]. By analogy, it is likely that $(CH_3)_2CHOC(O_2H)(CH_3)_2$ will decompose to form isopropyl hydroperoxide, $(CH_3)_2CHOOH$, and acetone:

$$(CH_3)_2CHOC(O_2H)(CH_3)_2 \rightarrow (CH_3)_2CHOOH + CH_3C(O)CH_3 \quad (23)$$

No evidence for this compound was found in the FT-IR spectra obtained in the small reactor and at EUPHORE. However, as indicated above, the characteristic absorption bands for hydroperoxides would be obscured by those of H_2O_2 and water, which are present in much larger quantities in the chamber. Isopropyl hydroperoxide may, however, be photolysed by UV light:

$$(CH_3)_2CHOOH + h\nu \rightarrow (CH_3)_2CHO + OH \quad (24)$$

This yields an alkoxy radical which is identical in structure to that formed in reaction (4b) and will react with O_2 to form acetone, reaction (8). Isopropyl hydroperoxide could also undergo reaction with OH radicals. H-atom abstraction from the $-O_2H$ group would produce the species $(CH_3)_2CHOO$ which would simply react with HO_2 to reform the hydroperoxide. Attack at the tertiary C–H bond would produce the alkyl radical $(CH_3)_2COOH$ which is presumably oxidised to produce acetone. The decomposition of isopropyl hydroperoxide is thus a possible secondary source of acetone and could help explain the secondary production of acetone observed in the H_2O_2 experiment performed in the small reactor (Fig. 6).

Since it was not possible to identify any of the hydroperoxides by FT-IR spectroscopy, neither of the above reaction pathways can be confirmed or dismissed. Nevertheless, it is clear that acetone production from the reaction or decomposition of

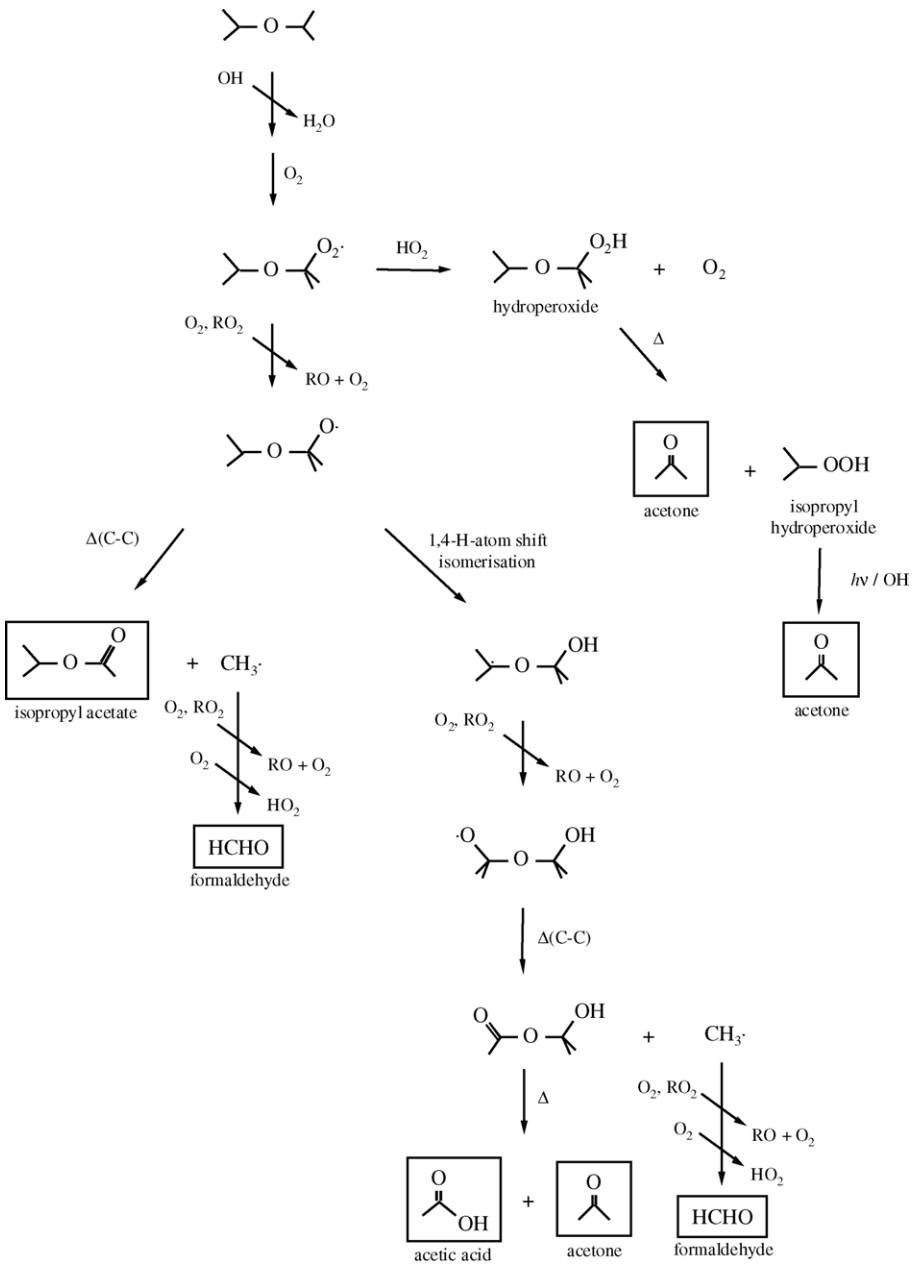

Fig. 8. Mechanism for the oxidation of diisopropyl ether in the absence of NO_x.

hydroperoxides is the major feature of the photooxidation of DIPE under conditions where $RO_2 + HO_2$ reactions dominate. The complete conversion of hydroperoxides to acetone would result in a yield of 200%. However, the yield of acetone in the "NO_x free" experiments performed at EUPHORE and in the small reactor is in the range 55–115%, indicating that a significant part of the carbon is in the form of hydroperoxides.

The photooxidation of DIPE in the absence of NO_x is complicated because both peroxy–peroxy ($RO_2 + RO_2$) and peroxy–hydroperoxy ($RO_2 + HO_2$) radical reactions can take place. In the experiments where H_2O_2 and $O_3/H_2O/CH_3OH$ were used to generate OH radicals, the $RO_2 + HO_2$ reactions dominate and acetone, arising from decomposition of the resulting hydroperoxides, is observed as the major reaction product. Under conditions where the $RO_2 + RO_2$ reactions dominate, $(CH_3)_2CHOC(O)(CH_3)_2$ radicals are produced. However, the $(CH_3)_2CHOC(O)(CH_3)_2$ radicals appear to behave differently to those produced from the $RO_2 + NO$ route. Since isopropyl acetate, acetone and acetic acid and formaldehyde are all detected as reaction products then the alkoxy radical can possibly undergo two out of the four possible reaction pathways: (i) C–C bond fission to produce isopropyl acetate and methyl radicals which generate formaldehyde, (ii) 1,4-H-atom isomerisation to yield acetic acid, acetone and formaldehyde. Based on the results obtained in this work, a mechanism for the photooxidation of DIPE in the absence of NO_x can be proposed (Fig. 8).

One particularly interesting mechanistic feature in the photooxidation of DIPE is the significant change in the relative

importance of the competing reaction pathways for the major alkoxy radical $(CH_3)_2CHOC(O)(CH_3)_2$. When the radical is produced by the $RO_2 + NO$ reaction, C–C bond fission is the dominant pathway. However, when the radical is produced via $RO_2 + RO_2$ reactions, the C–C bond fission channel diminishes in importance and 1,4-H-atom isomerisation takes over as the major reaction pathway. A similar variation in the reactions of alkoxy radicals in the presence and absence of NO_x has been observed for a number of other compounds [16,18,23–28] and can be explained on thermochemical grounds. The reactions of peroxy radicals with NO are exothermic [29] and proceed through an energy-rich peroxy nitrite intermediate, $ROONO^*$ [30]. This intermediate will either undergo O–O bond scission to form the alkoxy radical and NO_2 or form an organic nitrate. Since the self-reactions of peroxy radicals are close to thermoneutral [10], the heats of formation of RO_2 and RO may be assumed to be equal, and therefore the enthalpy change, ΔH, for the $RO_2 + NO$ reaction is equal to the difference between the heats of formation of NO and NO_2 (i.e. $-14\,kcal\,mol^{-1}$ [31]). This excess energy will be acquired by the peroxy nitrite intermediate and will be distributed within the complex and consequently between the products. In the case of DIPE photooxidation, the bulk of the excess energy is expected to be acquired by the $(CH_3)_2CHOC(O)(CH_3)_2$ radical thus making it chemically activated or "hot". Since the activation energy for C–C bond fission will be higher than that for 1,4-H-atom isomerisation, the chemically activated alkoxy radical is considerably more likely to undergo C–C bond fission than the thermoneutral alkoxy radical created via the peroxy self-reaction, which mainly reacts via the 1,4-H-atom isomerisation channel.

Finally, it is instructive to return to the concentration–time profile produced from the "classic NO_x" experiment shown in Fig. 1. As described above, there are three possible fates for the peroxy radicals formed following abstraction of the tertiary H-atom in diisopropyl ether: (1) reaction with NO to form chemically activated alkoxy radicals, (2) reaction with peroxy radicals, leading mainly to the formation of thermoneutral alkoxy radicals and (3) reaction with HO_2 to form a hydroperoxide. These three regimes are clearly represented in Fig. 1:

- 9:30–11:30 h. The high concentration of NO means chemically activated alkoxy radicals are formed via the $RO_2 + NO$ reaction. These undergo "prompt" decomposition by C–C bond scission to yield isopropyl acetate and formaldehyde as the major products.
- 11:30–13:30 h. As the concentration of NO decreases, peroxy–peroxy radical reactions become significant. The alkoxy radicals formed can: (i) decompose by C–C bond scission to yield isopropyl acetate and formaldehyde, (ii) isomerise to yield acetic acid, acetone and formaldehyde. Since formaldehyde can be formed as a result of both C–C bond scission and isomerisation, its yield increases relative to that of isopropyl acetate.
- 13:30–15:30 h. The concentration of HO_2 radicals has built up to a concentration where their reaction with the peroxy radical to form a hydroperoxide will dominate. The major fate of this hydroperoxide appears to be decomposition to form acetone, although the mechanism for this decomposition is not clear. Since alkoxy radical formation is now negligible, the formation of isopropyl acetate and formaldehyde is suppressed.

Acknowledgements

Financial support for this work was provided by the European Commission through the research project EUROSOLV (contract no. ENV4-CT97-0414) and the National funding agencies in Ireland and France. The authors would like to thank Manuel Pons (CEAM) and Lars Thuener (Wuppertal) for their assistance and valuable discussions during the course of this work.

References

[1] R. Atkinson, J. Phys. Chem. Ref. Data, Monograph No. 2, 1994.
[2] A. Mellouki, G. LeBras, H. Sidebottom, Chem. Rev. 103 (2003) 5077–5096.
[3] K.H. Becker (Ed.), The European Photoreactor EUPHORE, Final Report of theEC-Project, Contract EV5V-CT92-0059; Wuppertal, Germany, 1996.
[4] B. Klotz, S. Sørensen, I. Barnes, K.H. Becker, T. Etzkorn, R. Volkammer, U. Platt, K. Wirtz, M. Martín-Reviejo, J. Phys. Chem. 102 (1998) 10289–10299.
[5] R. Volkammer, U. Platt, K. Wirtz, J. Phys. Chem. A 105 (2001) 7865–7874.
[6] I. Magneron, R. Thévenet, A. Mellouki, G. LeBras, G.K. Moortgat, K. Wirtz, J. Phys. Chem. A 106 (2002) 2526–2537.
[7] J.C. Wenger, S. Le Calvé, H.W. Sidebottom, K. Wirtz, M. Martín-Reviejo, J.A. Franklin, Environ. Sci. Technol. 38 (2004) 831–837.
[8] J. Wenger, E. Collins, E. Porter, J. Treacy, H. Sidebottom, Chemosphere 38 (1999) 1197–1204.
[9] T.J. Wallington, J.M. Andino, A.R. Potts, S.J. Rudy, W.O. Siegl, Z. Zhang, M.J. Kurylo, R.E. Hule, Environ. Sci. Technol. 27 (1993) 98–104.
[10] R. Atkinson, Int. J. Chem. Kinet. 29 (1997) 99–111.
[11] T.J. Wallington, S.M. Japar, Environ. Sci. Technol. 25 (1991) 410.
[12] J. Eberhard, M. Semadeni, D.W. Stocker, J.A. Kerr, in: P. Borrell, et al. (Eds.), Proceedings of the Eurotrac Symposium '92, Garmisch-Partenkirchen, Germany, SPB Academic Publishing Co., The Hague, 1992.
[13] J. Eberhard, C. Müller, D.W. Stocker, J.A. Kerr, Int. J. Chem. Kinet. 25 (1993) 639.
[14] S.A. Cheema, K.A. Holbrook, G.A. Oldershaw, D.P. Starkey, R.W. Walker, Phys. Chem. Chem. Phys. 1 (1999) 3243.
[15] K. Stemmler, W. Mengon, J.A. Kerr, J. Chem. Soc., Faraday Trans. 93 (1997) 2865.
[16] J.J. Orlando, G.S. Tyndall, M. Bilde, C. Ferranto, T.J. Wallington, L. Vereecken, J. Peeters, J. Phys. Chem. A 102 (1998) 8116.
[17] L. Vereecken, J. Peeters, J. Phys. Chem. A 103 (1999) 1768.
[18] L. Vereecken, J. Peeters, J.J. Orlando, G.S. Tyndall, C. Ferranto, J. Phys. Chem. A 103 (1999) 4693.
[19] D.F. Smith, T.E. Kleindienst, E.E. Hudgens, C.D. McIver, J.J. Bufalini, Int. J. Chem. Kinet. 23 (1991) 907.
[20] E.C. Tuazon, W.P.L. Carter, S.M. Aschmann, R. Atkinson, Int. J. Chem. Kinet. 23 (1991) 1003.
[21] D.F. Smith, T.E. Kleindienst, E.E. Hudgens, C.D. McIver, J.J. Bufalini, Int. J. Chem. Kinet. 24 (1992) 199.
[22] H.H.K. Kurth, S. Gäb, W.V. Turner, A. Kettrup, Anal. Chem. 63 (1991) 2586.
[23] T.J. Wallington, M.D. Hurley, J.M. Fracheboud, J.J. Orlando, G.S. Tyndall, J. Sehested, T.E. Møgelberg, O.J. Nielsen, J. Phys. Chem. 100 (1996) 18116.
[24] T.E. Møgelberg, J. Sehested, G.S. Tyndall, J.J. Orlando, J.M. Fracheboud, T.J. Wallington, J. Phys. Chem. A 101 (1997) 2828.

[25] M. Bilde, T.J. Wallington, C. Ferranto, J.J. Orlando, G.S. Tyndall, E. Estupiñan, S. Haberkorn, J. Phys. Chem. A 102 (1998) 1976.
[26] M. Bilde, J.J. Orlando, G.S. Tyndall, T.J. Wallington, M.D. Hurley, E.W. Kaiser, J. Phys. Chem. A 103 (1999) 3963.
[27] L.P. Thüner, I. Barnes, K.H. Becker, T.J. Wallington, L.K. Christensen, J.J. Orlando, B. Ramacher, J. Phys. Chem. A 103 (1999) 8657.
[28] A.S. Hasson, I.W.M. Smith, J. Phys. Chem. A 103 (1999) 2031.
[29] W.B. DeMore, S.P. Sander, D.M. Golden, R.F. Hampson, M.J. Kurylo, C.J. Howard, A.R. Ravishankara, C.E. Kolb, M.J. Molina, J.P.L. Publication '97-4, 1997.
[30] M.M. Maricq, J.J. Szente, J. Phys. Chem. 100 (1996) 12374.
[31] S.W. Benson, Thermochemical Kinetics, 2nd ed., Wiley, New York, 1976.